

Emodin Ameliorates Renal Damage and Podocyte Injury in a Rat Model of Diabetic Nephropathy via Regulating AMPK/mTOR-Mediated Autophagy Signaling Pathway

This article was published in the following Dove Press journal:
Diabetes, Metabolic Syndrome and Obesity: Targets and Therapy

Hong Liu^{1,*}
Quan Wang^{1,*}
Ge Shi¹
Wenqiang Yang²
Yanmin Zhang¹
Weidong Chen¹
Sheng Wan¹
Fei Xiong¹
Zengsi Wang¹

¹Department of Nephrology, Wuhan No. 1 Hospital, Wuhan, Hubei, 430022, People's Republic of China; ²Department of Central Laboratory, Wuhan No. 1 Hospital, Wuhan, Hubei, 430022, People's Republic of China

*These authors contributed equally to this work

Correspondence: Fei Xiong; Zengsi Wang
Department of Nephrology, Wuhan No. 1 Hospital, No. 215 Zhongshan Avenue, Wuhan, Hubei, 430022, People's Republic of China
Tel +86-27-85332356;
+86-27-85332346
Email xiongf23@sina.com;
wangzengsi@hotmail.com

Purpose: The activation of autophagy has potential protective effect on diabetic nephropathy (DN) podocyte injury, and the AMPK/mTOR signaling pathway is an important regulatory pathway of autophagy. Emodin has been reported to effectively delay DN progression; however, the therapeutic mechanisms involved in vivo remain ambiguous. The present study aimed to elucidate the mechanism of emodin in improving renal tissue and podocyte injury in DN by regulating the AMPK/mTOR-autophagy signaling pathway.

Methods: All rats were divided into 4 groups: a Sham group, a Vehicle group, a low-dose emodin (LD-Emo) group (20 mg/kg/day) and a high-dose emodin (HD-Emo) group (40 mg/kg/day). The different doses of Emo and distilled water were daily administrated for 8 weeks after the induction of DN by the unilateral nephrectomy combined with intraperitoneal injections of streptozotocin (STZ). The rats' general status, blood glucose, biochemical parameters, urinary protein excretion, renal histological changes and cell apoptosis in renal tissue, as well as the key protein expressions in the AMPK/mTOR signaling pathway and apoptosis-related proteins were examined, respectively.

Results: Emodin ameliorated the general condition, kidney weight and urinary protein excretion of the rats, but has little influence on serum biochemical parameters and did not lower blood glucose; emodin attenuated renal fibrosis including the cell numbers, extracellular matrix rate and collagen area in glomerulus, simultaneously relieved podocyte foot process fusion, up-regulated the expression of nephrin protein and suppressed glomerular and tubular epithelial cell apoptosis. In addition, emodin can induce and enhance autophagy in podocytes including increased expression of LC3-II/I, Beclin-1, p-AMPK protein and decreased expression of p62, p-mTOR protein, as well as increased autophagosomes in podocytes.

Conclusion: We have demonstrated that emodin, as a natural regulator in vivo, reduced proteinuria and alleviated renal fibrosis without affecting hyperglycemia in DN rats. The potential mechanisms by which emodin exerts its renoprotective effects in vivo are through suppressing cell apoptosis and enhancing autophagy of podocytes via the AMPK/mTOR signaling pathway in the kidney.

Keywords: emodin, diabetic nephropathy, autophagy, cell apoptosis, AMPK/mTOR signaling pathway

Introduction

Diabetic nephropathy (DN) is a serious microvascular complication of diabetes mellitus, which has become the main cause of end-stage renal disease (ESRD) and

has brought heavy economic burden to the whole society.¹ Therefore, the development of novel approaches for treatment of DN is urgently needed. Podocytes are terminally differentiated glomerular epithelial cells, which reside on the glomerular basement membrane (GBM) outside the glomerular capillaries. Proteinuria is a significant clinical feature of DN and usually associates with different degrees of podocyte injury.² Nephlin is a main podocyte cytoskeletal protein and slit diaphragm structural protein, which plays a key role in maintaining the integrity and normal function of glomerular filtration barrier by regulating the structure and function of podocytes.³ The abnormal expression and function of nephlin in diabetic patients may damage the integrity of renal filtration membrane structure and barrier function, and participate in the production of diabetic glomerulosclerosis and proteinuria.

Autophagy is the self-degradation of lysosome-dependent macromolecular proteins and organelles that provides raw materials and nutrition for cell repair, and realizes organelle renewal by scavenging senescent organelles and long-lived proteins.⁴ Apoptosis is a programmed method of gene regulation and biological autonomy in order to maintain a constant number of cells. At present, it has been confirmed that autophagy exists in the process of apoptosis, and there is a certain relationship between autophagy and apoptosis. The same stimulus can cause autophagy and apoptosis at different intensities. Podocytes, as terminal differentiated cells, have limited regenerative capacity. Under the stimulation of various stress factors in the process of DN, a large number of damaged proteins and organelles accumulate in podocytes, which will lead to podocyte loss and podocyte apoptosis. Studies have found that podocytes maintain the basic level of autophagy under normal conditions,⁵ while autophagy activity is significantly increased after podocytes are damaged.⁶ Therefore, there is a close relationship between autophagy and apoptosis in podocytes. Podocyte autophagy deficiency is an important trigger point of proteinuria, while maintaining a certain level of autophagy can reduce the occurrence of apoptosis.

Emodin is an anthraquinone derivative with a chemical name of 1,3,8-trihydroxy-6-methylanthraquinone, which is the main effective monomer of rhubarb in traditional Chinese medicine.⁷ Pharmacological studies have demonstrated that emodin has pharmacological effects such as anti-bacterial,⁸ anti-inflammation,⁹ anti-oxidation,¹⁰ immunosuppression,¹¹ anti-renal fibrosis,¹² anticancer,¹³ etc. Rhubarb, as a traditional Chinese medicine, has a extensive pharmacological effects, and rhubarb preparations have been widely used in

clinical treatment of DN. Emodin, as the main active ingredient of rhubarb, has been reported to inhibit cell proliferation and fibronectin expression by inhibiting the p38 MAPK pathway in vivo and in vitro.^{14,15} Another study showed that emodin treated early DN by inhibiting high glucose-induced podocyte transdifferentiation, increasing nephlin protein expression and reducing proteinuria.¹⁶ But in general, there is not much research of the pharmacological mechanism of emodin on its protection in DN podocyte injury; similarly, it is unclear whether the underlying mechanism of emodin in the treatment of DN is associated with podocyte autophagy. Studies have reported that the pathogenesis of DN is related to nutritional sensitive pathways such as the mammalian target of rapamycin (mTOR) and AMP activated protein kinase (AMPK) signaling pathway.¹⁷ And autophagy can be promoted by AMPK, while it is inhibited by mTOR; AMPK promotes autophagy by directly activating Ulk1 through phosphorylation of Ser 317 and Ser 777, under nutrient sufficiency, while the high activity of mTOR prevents Ulk1 activation by phosphorylating Ulk1 Ser 757 and disrupting the interaction between Ulk1 and AMPK.¹⁸ It has been reported that emodin is an effective AMPK activator,¹⁹ and our previous studies have shown that emodin ameliorates cisplatin-induced apoptosis of rat renal tubular cells in vitro through modulating the AMPK/mTOR signaling pathways and activating autophagy.⁷ Whether emodin can effectively protect podocyte injury in DN, and whether it is related to the AMPK/mTOR-autophagy signaling pathway, is not clear.

Hence, in this study, we established a rat model of DN by unilateral nephrectomy combined with intraperitoneal injection of streptozotocin (STZ). We tried to elucidate the mechanism of emodin in improving renal tissue and podocyte injury in DN by regulating the AMPK/mTOR-autophagy signaling pathway. It provides a new target for emodin in the treatment of DN, and also provides a novel and effective therapeutic method for DN patients.

Materials and Methods

Reagents, Drug and Animals

Emodin (MB5674, HPLC $\geq 98\%$) was purchased from Dalian Meilun Biotechnology Co., Ltd (Dalian, China). Emodin was dissolved in 0.5% sodium carboxymethyl cellulose and prepared into emodin suspension (10 mg/mL). Streptozotocin (STZ, CAS#: 18883-66-4) was purchased from Aladdin Reagent Co., Ltd (Shanghai, China). Apoptosis was detected by terminal deoxynucleotidyl transferase (TdT)-mediated deoxyuridine triphosphate (dUTP)-

biotin nick end labeling (TUNEL) assay with a detection kit (Cat. No. 11684817910; Roche, Switzerland). Blood glucose meter and blood glucose test paper were purchased from 3Nod Electronics Co., Ltd (Shenzhen, China).

All experiments were performed using male Sprague-Dawley (SD) rats, aged 8 weeks and weighing 200 ± 20 g, purchased from Experimental Animal Center of China Three Gorges University (Qualified by Hubei Center for Disease Control and Prevention, Wuhan, Hubei Province, China). Rats were kept in an environmentally controlled breeding room (temperature: $23^{\circ}\text{C}\pm 2^{\circ}\text{C}$, humidity: $60\%\pm 5\%$, a 12-hour light/dark cycle), and fed a standard rat chow and given tap water ad libitum in the Experimental Animal Center of Wuhan Servicebio Technology Co., Ltd (Wuhan, China). They were acclimatized for 1 week before the experiment. The surgical procedures and experimental protocol were approved by the Animal Ethics Committee of Wuhan No. 1 Hospital and complied with ethical standards in Laboratory Animal – Guideline for Ethical Review of Animal Welfare (The National Standard of the People's Republic of China GB/T 35892-2018).

Experimental Design

The experimental procedure is illustrated in Figure 1. The DN model in rats was established by unilateral nephrectomy combined with STZ intraperitoneal injections with low doses of 35 mg/kg BW twice at 72-hour interval.²⁰ We collected blood through the tail vein, and then used the blood glucose meter to detect the blood glucose of rats. Twenty-six rats were randomly divided into 4 groups: 5

rats in a Sham operation group (Sham operation + distilled water), 7 rats in a Vehicle group (DN + distilled water), 7 rats in a low-dose emodin (LD-Emo) group (DN + low-dose of emodin suspension), 7 rats in a high-dose emodin (HD-Emo) group (DN + high-dose of emodin suspension). According to previous studies,^{16,21,22} 20 mg/kg and 40 mg/kg of emodin suspension were respectively given in LD-Emo group and HD-Emo group by gavage every day. Sham operation and Vehicle group were given equal amounts of distilled water by gavage every day for 8 weeks. The rats were weighed weekly, and the dosage was adjusted. After 8 weeks of administration, all rats were anesthetized by intraperitoneal injection of ketamine and sacrificed through cardiac puncture. Blood samples and kidneys were collected for detection of various indicators.

General Status, Blood Glucose, Urinary Albumin and Urinary Creatinine Ratio (Urinary ACR)

The spirit, diet, drinking water, fur color, defecation and activities of the rats in each group were observed every day. Body weight (BW), blood glucose (BG) and urinary ACR of rats were detected respectively before and every 2 weeks after modeling. At the end of 8 weeks of administration, the rats were weighed. The appearance and morphology of the kidney were observed and photographed. After the kidney was removed, the kidney weight (KW) was recorded, and the kidney weight/body weight (KW/BW) was calculated.

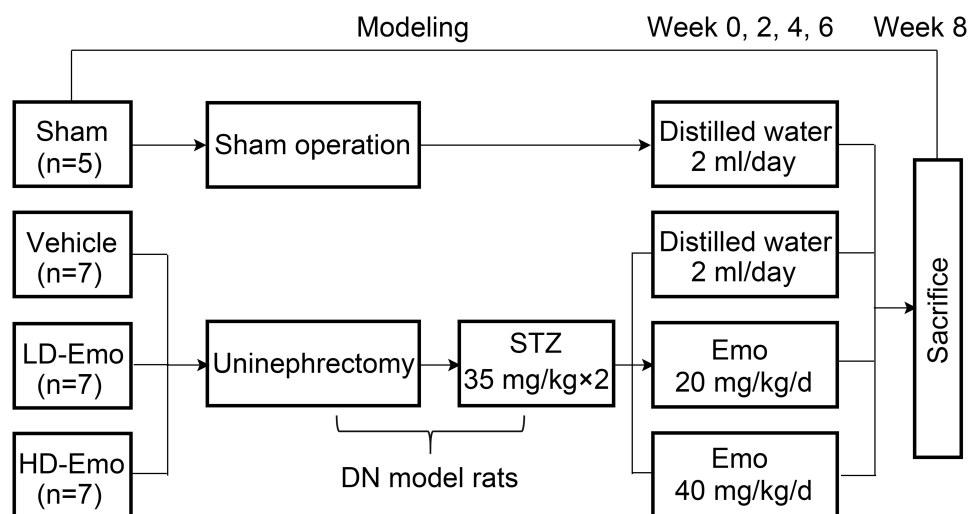


Figure 1 Experimental procedure.

Abbreviations: Sham, Sham operation + distilled water group; Vehicle, DN + distilled water group; LD-Emo, DN + low-dose emodin group; HD-Emo, DN + high-dose emodin group; DN, diabetic nephropathy; STZ, streptozotocin.

Serum Biochemical Parameters

After 8 weeks of administration, rats were anesthetized with ketamine, the thoracic cavity was dissected and 5 mL of blood was collected through the heart. Serum indicators including albumin (Alb), blood urea nitrogen (BUN), serum creatinine (Scr), uric acid (UA), total cholesterol (TC) and triglyceride (TG) were detected by automatic biochemical analyzer (Laboratory Department of Wuhan No. 1 Hospital).

Renal Histology

The abdominal cavities of rats were carefully incised, and then the right kidney was removed from renal hilum. After removing the kidney, renal cortex and medulla were separated. A small amount of renal cortex at both renal poles was taken and fixed in 10% neutral buffered formalin, dehydrated for 16 h, embedded in paraffin, cut into 3- μ m-thick slices, and periodic acid Schiff (PAS) staining and Masson staining were performed. The number of glomerular cells, extracellular matrix (ECM) and collagen deposition were observed by light microscopy. Twenty glomeruli of each section were selected randomly, and the cell numbers, the relative area of ECM and collagen in glomeruli were calculated with Image-Pro Plus 6.0 software (Media Cybernetic, Washington, USA).

Electron Microscopy

Renal tissue samples for electron microscopic assessment were fixed in 2.5% glutaraldehyde in 0.1 mol/L phosphate buffer (PB) for several days at 4°C. After washing in PB and post-fixing in 1% OsO₄ for 2 h, the fixed material was dehydrated through an ethanolpropylene oxide series and embedded in Araldite M. The ultrathin sections were prepared and stained with uranyl acetate and lead citrate. Transmission electron microscopy was performed using transmission electron microscope HT7800 (HITACHI, Japan) in the Ultrastructural Pathology Center of Renmin Hospital of Wuhan University.

TUNEL Assay

The sections were stained according to the manufacturer's protocol for paraffin-embedded tissues. The sections were heated at 65°C for 2 h, and then deparaffinization was performed, followed by washing in 2 changes of xylene, 15–20 min each. The tissue sections were dehydrated in 2 changes of pure ethanol for 10 min each, followed by dehydration in gradient ethanol of 95%, 90%, 80% and 70% ethanol, respectively, 5 min each and washed in

distilled water. They were then incubated with 20 μ g/mL proteinase K solution at 37°C for 25 min and washed three times with PBS, 5 min each. And then the tissues were immersed in 3% hydrogen peroxide in methanol for 15 min to block endogenous peroxidase activity and were washed again with PBS. TUNEL reaction: Mix reagent 1 (TdT) and reagent 2 (dUTP) (both from the TUNEL assay kit) at a ratio of 1:9. Prepare this reaction solution according to demand before use. Add this mixture to objective tissue placed in a flat wet box, incubate at 37°C for 2 h in a moist and dark environment. The tissues were then washed three times with PBS, 5 min each. Subsequently, the tissues were incubated with DAPI solution at room temperature for 10 min, kept in dark place. And then they were washed three times again with PBS, 5 min each. Some of the liquid was discarded, then a coverslip with anti-fade mounting medium was applied. Microscopy detection was performed and images collected by Fluorescent Microscopy. DAPI glows blue by UV excitation wavelength 330–380 nm and emission wavelength 420 nm; FITC glows green by excitation wavelength 465–495 nm and emission wavelength 515–555 nm; CY3 glows red by excitation wavelength 510–560 nm and emission wavelength 590 nm. Nucleus is blue by labeling with DAPI. TUNEL assay kit is from Roche and labeled with FITC. Positive apoptosis cells are green.

Western Blot Analysis

Western blot analysis was performed using the following antibodies: anti-rat nephrin (ab58968), anti-rat AMPK (ab80039), anti-rat p-AMPK (ab23875), anti-rat β -actin (ab227387) antibodies were from Abcam Ltd, HKSP, New Territories, HK; anti-rat LC3 I/II (12741), anti-rat Beclin-1 (3495), anti-rat mTOR (2983), anti-rat p-mTOR (5536), anti-rat Cleaved caspase3 (9661) antibodies were from Cell Signaling Technology Company, Beverly, MA, USA; anti-rat p62 (A19700) antibodies were from ABclonal Biotechnology Co., Ltd, Wuhan, China; anti-rat Bax (GB11007) antibodies were from Servicebio Technologies Co., Ltd, Wuhan, China; anti-rat caspase3 (BM4620) antibodies were from Boster Biological Technology Co., Ltd, Wuhan, China. Horseradish peroxidase (HRP)-conjugated anti-rabbit immunoglobulins and anti-mouse immunoglobulins were from KPL Company, USA.

Renal cortex samples (100 mg) were washed by phosphate-buffered saline and centrifugated for 3 to 5 times. Total protein lysate that contains protease inhibitors and

phosphatase inhibitors was used for extracting the total protein. Lysate protein concentrations were determined by bicinchoninic acid (BCA) protein concentration assay kit (Beyotime Biotechnology, Shanghai, China). The total protein was mixed with 5×electrophoresis sample buffer (Beyotime Biotechnology, Shanghai, China). Equal amounts of protein in each sample were subjected to sodium dodecyl sulfate-polyacrylamide gel electrophoresis (SDS-PAGE) with 10% acrylamide gels, and then electrophoretically transferred to polyvinylidene fluoride membrane (Millipore, Bedford, USA). The membranes were blocked with 5% skimmed milk in tris-buffered saline-Tween-20 (TBS-T). The blots were incubated with primary antibodies (diluted according to the manufacturer's instructions). They were washed with tris-buffered saline-tween (TBST) and incubated with HRP-conjugated anti-rabbit or anti-mouse immunoglobulins. The membranes were coated using HRP-labeled chemiluminescent substrates (Millipore, Bedford, USA), eventually exposed and fixed in the dark box. This procedure was carried out 3 times. The results were quantified using Image-Pro Plus 6.0 software (Media Cybernetic, Washington, USA), which were contrasted with densitometric signal of β -actin, respectively, and the ratios were expressed as the relative protein contents.

Statistical Analyses

The results were expressed as mean \pm SEM. Statistical analysis was performed using one-way analysis of variance (ANOVA); LSD method was used for multiple comparison. $P < 0.05$ was defined as statistically significant. All data were analyzed using statistical software SPSS 24.0.

Results

Emodin Ameliorates the General Status and Renal Morphological Appearance in Rats with DN

During the experiment, in addition to the sham-operated rats, the other three groups of DN rats exhibited increased diet, drinking and urine, low activity, dull fur and BW loss at different degrees; the rats in Vehicle group were most obvious. After drug intervention, low activity of rats was gradually ameliorated after the treatment with emodin at both low and highdose. Subsequently, BW of rats in emodin-treated groups increased gradually, at the end of 8 weeks of administration, in comparison with the rats in the Sham group, BW of DN rats declined ($P < 0.01$), and

in the emodin-treated groups, BW of rats was higher compared with those in the Vehicle group; there were significant differences among the three groups ($P < 0.05$) (Figure 2A).

The ratio of KW to BW in the Vehicle group was obviously higher than that in the Sham group ($P < 0.01$), while KW/BW of rats in the emodin-treated groups declined, and the differences were statistically compared with the Vehicle group ($P < 0.01$), but they were still higher than that in the Sham group, and there was statistically significant differences between the two treatment groups ($P < 0.05$) (Figure 2B). In addition, renal appearance in the Sham group was moderated and crimson, while those in Vehicle group were swollen and ischemic. The kidneys of rats treated with emodin at both low and high dose were significantly ameliorated, with less swelling and ischemia (Figure 2C). In sum, these results showed that emodin could ameliorate the rat's general status and renal morphological appearance of DN rats, as well as influencing BW and KB/BW; all of these have little correlation to emodin dosage.

Emodin Can Ameliorate Urinary ACR, but Had No Significant Effect on Blood Glucose and Serum Biochemical Parameters

As shown in Figure 3A, at the end of 8 weeks of administration, urinary ACR in the Vehicle group reached an abnormal level (73.34 ± 5.15 mg/g), which was significantly higher than that in the Sham group (2.28 ± 0.27 mg/g) ($P < 0.01$), while the level of urinary ACR was significantly decreased in the LD-Emo group (17.02 ± 1.22 mg/g) and the HD-Emo group (14.23 ± 2.35 mg/g), and the difference reached statistical significance compared with the Vehicle group ($P < 0.01$), but there was no statistical difference between the LD-Emo group and the HD-Emo group ($P > 0.05$). After successful modeling, the BG of rats in the Vehicle group remained at a high level, and at the end of the 8th week of administration, the BG of rats in the Vehicle group (29.21 ± 0.81 mmol/L) was still very high; however, it is worth noting that BG of rats in the LD-Emo group (27.10 ± 1.13 mmol/L) and the HD-Emo group (26.70 ± 0.70 mmol/L) also remained at high levels, respectively, and the differences were statistically significant compared with the Sham group (6.88 ± 0.83 mmol/L) ($P < 0.01$), but there was no statistical difference between the Vehicle group and the emodin-treatment groups ($P > 0.05$) (Figure 3).

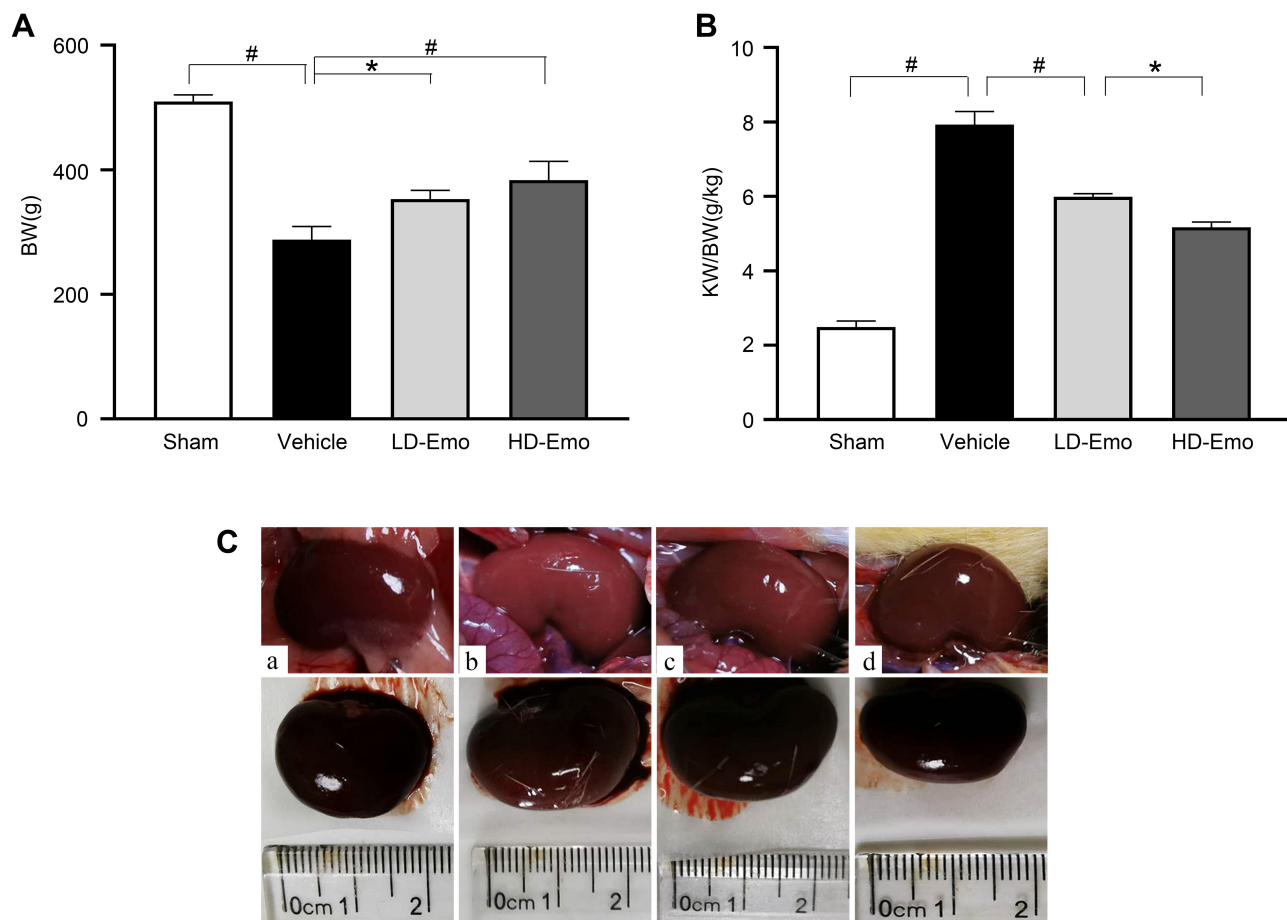


Figure 2 Effects of Emo on changes in body weight, kidney weight/body weight and renal appearance.

Notes: (A) body weight, (B) kidney weight/body weight, (C) renal appearance. (a) Sham group, (b) Vehicle group, (c) LD-Emo group, (d) HD-Emo group. Data are expressed as mean \pm SEM. * $P < 0.05$, # $P < 0.01$.

Abbreviations: Emo, emodin; BW, body weight; KW/BW, kidney weight/body weight; LD-Emo, low-dose emodin; HD-Emo, high-dose emodin.

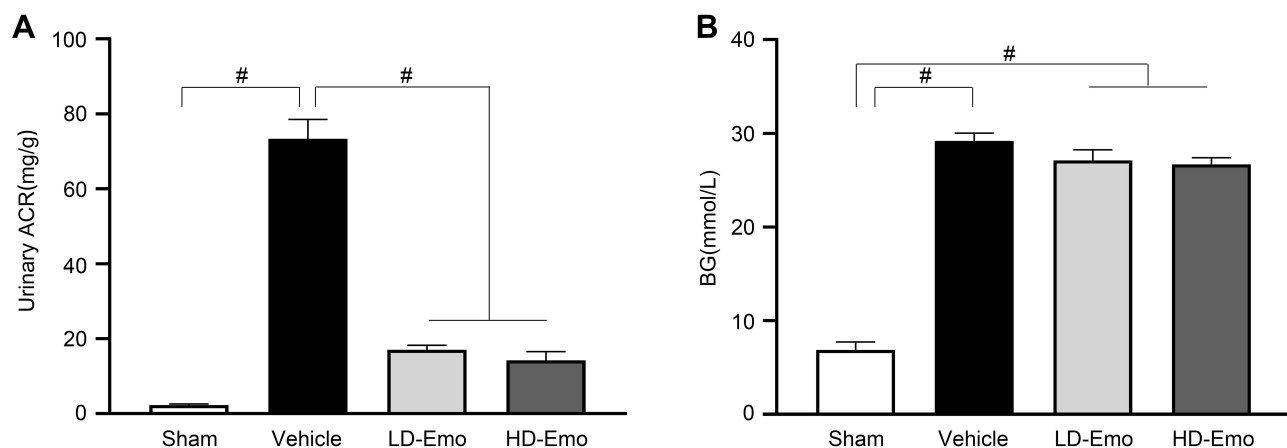


Figure 3 Effects of Emo on changes in urinary albumin/urinary creatinine ratio and blood glucose. Data are expressed as mean \pm SEM. # $P < 0.01$.

Notes: (A) Urinary albumin/urinary creatinine ratio, (B) blood glucose.

Abbreviations: Emo, emodin; Urinary ACR, urinary albumin/urinary creatinine ratio; BG, blood glucose; LD-Emo, low-dose emodin; HD-Emo, high-dose emodin.

Compared with the Sham group, Alb in the Vehicle group decreased significantly ($P < 0.01$), but both emodin-treatment groups did not improve Alb ($P > 0.05$).

BUN in the Vehicle group was dramatically increased ($P < 0.01$), and the increased BUN was decreased by emodin treatment in both the LD-Emo and the HD-Emo

group ($P < 0.01$). Scr and UA were increased in the Vehicle group; compared with the Vehicle group, Scr and UA in emodin-treatment groups decreased slightly, but there was no significant difference ($P > 0.05$). TC was increased in the Vehicle group and emodin-treatment groups ($P < 0.01$); there were no statistical differences among the three groups ($P > 0.05$). TG was increased in the Vehicle group ($P < 0.01$), and similarly there was no statistical difference between the Vehicle group and emodin-treatment groups ($P > 0.05$) (Table 1). In sum, these results showed that emodin could ameliorate urinary ACR, but could not lower BG and had no significant effect on serum biochemical parameters in DN model rats.

Effects of Emodin on Histological Changes in Rats with DN

We observed glomerular morphological changes by light microscopy among 4 groups of rats. As shown in Figure 4A and B, no pathological changes were observed under light microscopy in the Sham group. However in the Vehicle group, mesangial tissues were showing obvious signs of hyperplasia, including glomerular mildhypertrophy, capillary loop area reduction, glomerular cell proliferation, ECM expansion and diffused increasing ECM areas. With HD-Emo treatment, the injurious glomerular morphological changes were visibly attenuated, which was superior to the LD-Emo group. When compared with the Sham group, the cell numbers, rate of ECM and collagen area in glomerulus were significantly increased in the Vehicle group, respectively, but decreased in emodin-treated groups (Figure 4C–E). However, no significant differences of glomerular morphological changes were found between the LD-Emo group and the HD-Emo group.

In the Sham group, electron microscopy showed normal glomerular basement membrane and podocyte foot

process. But in the DN rats, the glomerular basement membrane was occasionally thickened. Besides, there were apparent fusion and effacement of most podocyte foot processes. However, the injury of podocyte was markedly relieved in the emodin-treated groups (Figure 4F).

Emodin Suppressed Glomerular and Tubular Epithelial Cell Apoptosis in Rats with DN

TUNEL staining and Western blot analysis were used to confirm the presence of apoptosis in diabetic rats and observe the effect of emodin on apoptosis. There were very few TUNEL-positive cells in the Sham group, but a higher level of glomerular and tubular epithelial cell apoptosis was detected in the Vehicle group. After emodin treatment, a marked decrease of TUNEL-positive cells was observed, indicating the suppression of glomerular and tubular epithelial cell apoptosis in rats with DN by emodin (Figure 5A–D). Western blot analysis showed that, in the Vehicle group, the expression of Bax and Cleaved caspase-3 increased. However, after the intervention with emodin, expression of Bax and Cleaved caspase-3 was significantly suppressed (Figure 6A–C).

Effects of Emodin on Renal Cortical Expression of Nephritin and Autophagy in Podocytes in Rats with DN

To determine whether the renoprotective effects of emodin are related to podocytes in diabetic rats, nephritin expression in the renal cortical expression was analysed by Western blot. As shown in Figure 7A and B, the expression of nephritin was significantly reduced in the Vehicle group. In parallel to the attenuation of proteinuria, the impaired expression of nephritin was visibly restored by the treatment with emodin. To clarify the role of autophagy in the renoprotective effects of emodin, we examined the expressions of microtubule-associated protein 1 light-chain 3 (LC3),

Table 1 Comparison of Blood Biochemical Parameters of Rats Among Groups at the end of 8 Weeks

Group	Sham (n = 5)	Vehicle (n = 7)	LD-Emo (n = 7)	HD-Emo (n = 7)
Alb (g/L)	28.06 ± 0.35	24.87 ± 0.60**	25.13 ± 0.30**	25.79 ± 0.49**
BUN (mmol/L)	5.36 ± 0.26	27.46 ± 1.86**	13.96 ± 1.64**,#	10.13 ± 1.64*,#
Scr (μmol/l)	35.80 ± 1.16	43.57 ± 3.33*	42.71 ± 1.95	42.29 ± 2.33
UA (μmol/L)	49.00 ± 3.78	61.00 ± 9.43	54.57 ± 3.57	52.29 ± 6.20
TC (mmol/L)	1.25 ± 0.05	1.75 ± 0.15**	1.73 ± 0.02**	1.71 ± 0.04**
TG (mmol/L)	0.23 ± 0.02	0.40 ± 0.03**	0.37 ± 0.02**	0.36 ± 0.03**

Notes: * $P < 0.05$, ** $P < 0.01$ vs Sham group. # $P < 0.01$ vs Vehicle group.

Abbreviations: Alb, albumin; BUN, blood urea nitrogen; Scr, serum creatinine; UA, uric acid; TC, total cholesterol; TG, triglyceride. Data are expressed as mean ± SEM.

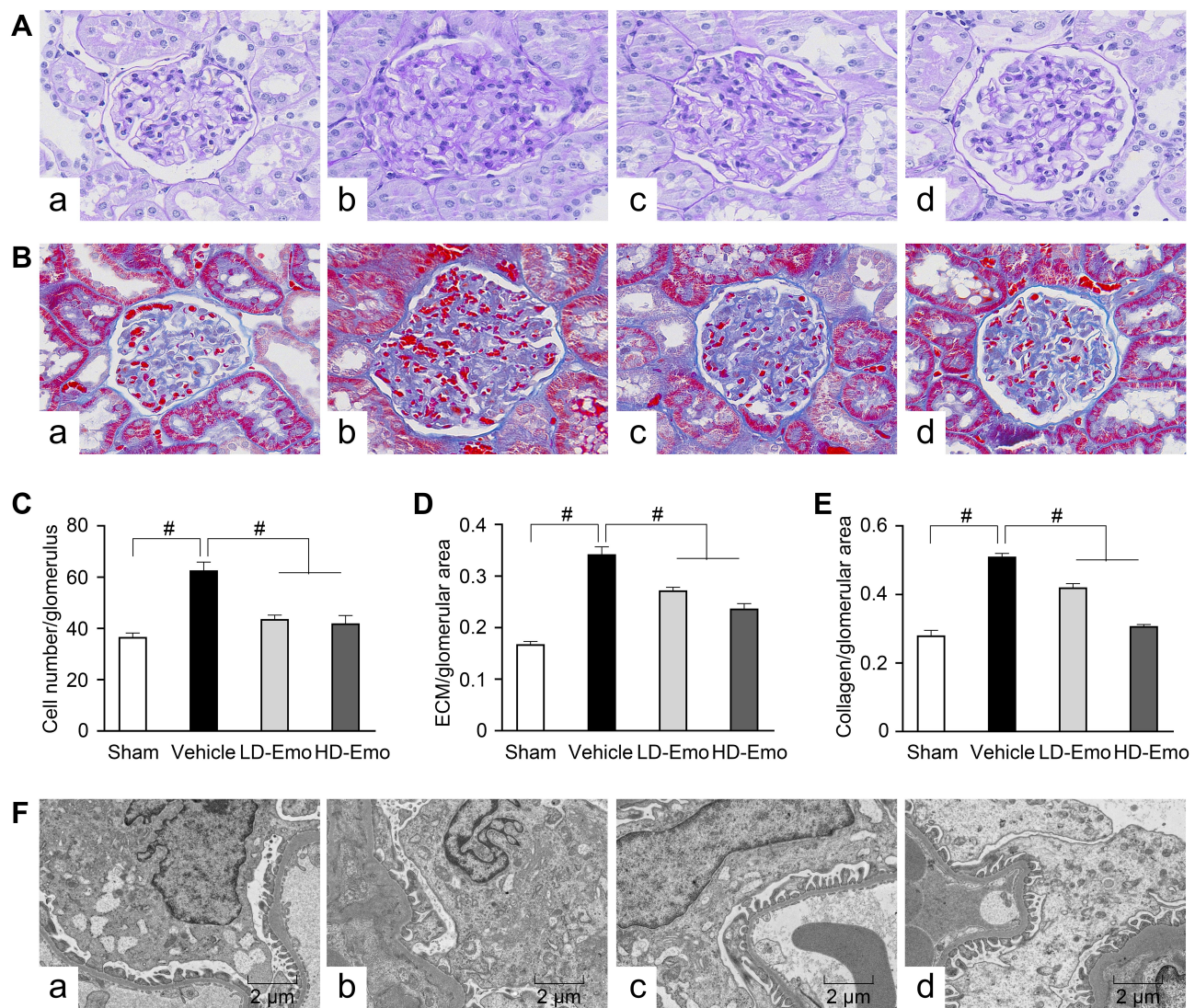


Figure 4 Effects of Emo on the glomerular morphological changes.

Notes: (A) Light microscopy, periodic acid-Schiff (PAS) staining (magnification, $\times 400$), (B) light microscopy, Masson staining (magnification, $\times 400$), (C) the number of glomerular cells, (D) the rate of ECM/glomerular area, (E) the rate of collagen/glomerular area, (F) electron microscopy, $5000\times$. (a) Sham group, (b) Vehicle group, (c) LD-Emo group, (d) HD-Emo group. Data are expressed as mean \pm SEM. [#] $P < 0.01$.

Abbreviations: Emo, emodin; ECM, extracellular matrix; LD-Emo, low-dose emodin; HD-Emo, high-dose emodin.

Beclin-1 and p62 protein by Western blot. The expression of LC3-II/I and Beclin-1 was significantly reduced in the Vehicle group, but was markedly increased in emodin-treated groups. Conversely, the expression of p62 protein exhibited the opposite trend (Figure 7A, C–E). Given the vital role of the AMPK/mTOR pathway in autophagy,¹⁸ we examined the influence of emodin on this pathway. Western blot analysis showed that the expression of p-AMPK protein was decreased in the Vehicle group, but was significantly increased in emodin-treated groups. Conversely, the expression of p-mTOR protein was induced in the Vehicle group, but was visibly inhibited by the treatment with emodin (Figure 7F–H).

In addition, we observed the autophagosomes in podocytes by transmission electron microscopy. A few autophagosomes were observed in the Sham group, but were absent in the Vehicle group; after intervention by emodin, autophagosomes increased gradually (arrow mark), suggesting that autophagy has a self-stabilizing effect and the renoprotective effects of emodin were associated with reversing insufficient autophagy in podocytes under diabetic conditions (Figure 8).

Discussion

In light of previous studies,²⁰ a diabetic nephropathy model was established by unilateral nephrectomy combined with

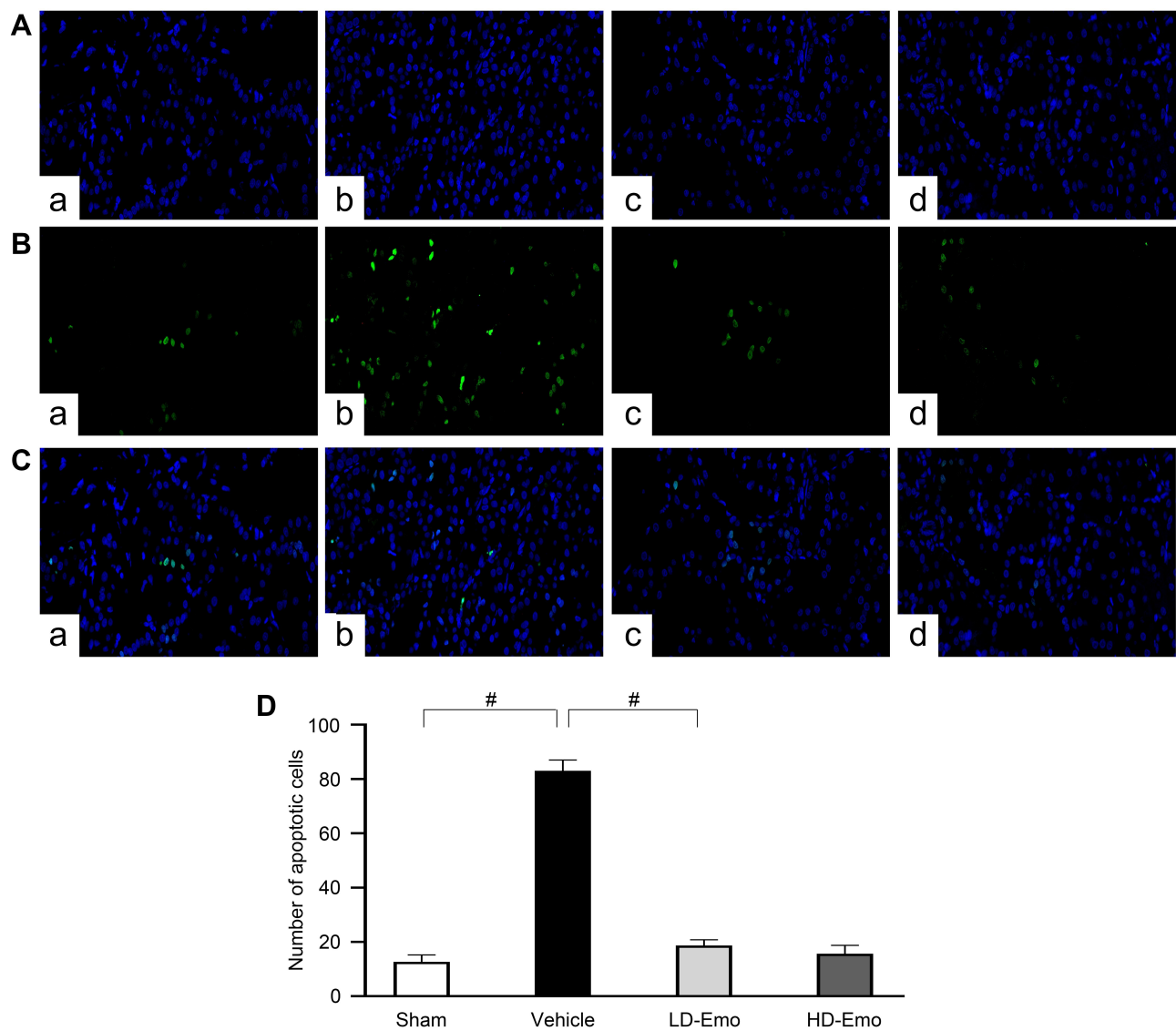


Figure 5 Effects of Emo on the glomerular and tubular epithelial cell apoptosis.

Notes: TUNEL staining (magnification, $\times 200$). **(A)** Nucleus is blue by labeling with DAPI, **(B)** positive apoptosis cells are green, **(C)** merging of **A** and **B**, **(D)** quantification of the number of apoptotic cells. (a) Sham group, (b) Vehicle group, (c) LD-Emo group, (d) HD-Emo group. Data are expressed as mean \pm SEM. $^{\#}p < 0.01$.

Abbreviations: Emo, emodin; TUNEL, terminal deoxynucleotidyl transferase (TdT)-mediated deoxyuridine triphosphate (dUTP)-biotin nick end labeling; LD-Emo, low-dose emodin; HD-Emo, high-dose emodin.

STZ intraperitoneal injections with low doses of 35 mg/kg BW twice at a 72-hour interval, a model which has stable hyperglycemia and typical pathological characteristics of renal fibrosis such as glomerular hypertrophy, glomerular cell proliferation and ECM deposition. In the present study, our data demonstrated that the increased urinary ACR in DN rats was significantly suppressed by emodin treatment. In addition, pathological changes to glomerular as well as damaged podocytes were visibly attenuated with the treatment of emodin. Nevertheless, emodin had no effect on hyperglycemia in these DN model rats, suggesting that the renoprotective effects of emodin were independent of BG control.

Proteinuria is an important risk factor and predictor of the progression of renal diseases.²³ The damage of podocyte foot processes structure plays an important role in the impaired glomerular filtration and proteinuria.²⁴ In DN, podocyte injury, which is closely related to proteinuria, includes podocyte fusion, podocyte number or density reduction and podocyte apoptosis.^{25,26} These pathological changes are not only an important factor in the progression of DN, but also a key target of drug therapy. Our results showed apparent fusion and effacement of most podocyte foot processes in the Vehicle group, which were markedly relieved in the emodin-treated groups. Nephrin is a main

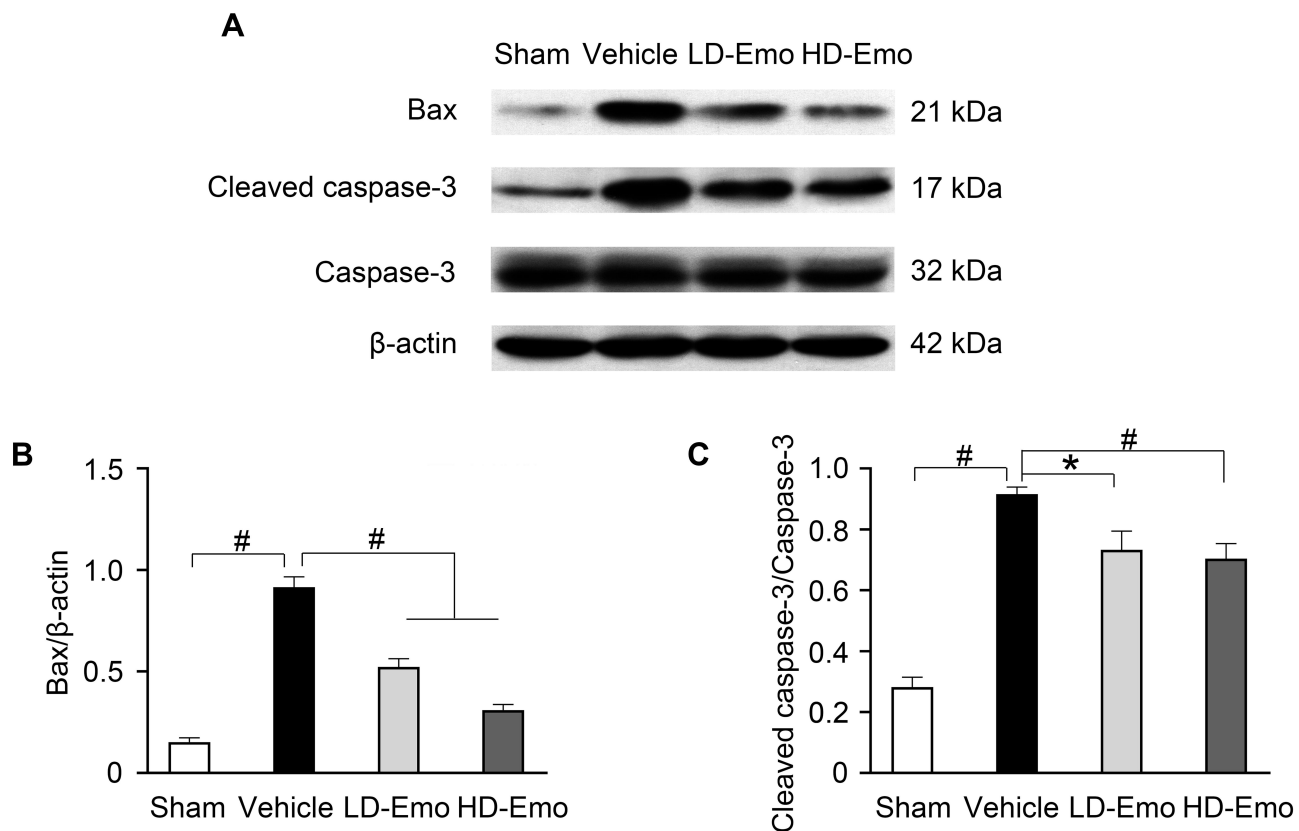


Figure 6 Effects of Emo on the protein expression of Bax and Cleaved caspase-3 in the kidney.

Notes: (A) Western blot analysis of Bax, Cleaved caspase-3 and caspase-3 protein expression. (B and C) Quantitative analysis of Bax and Cleaved caspase-3 protein expression. Data are expressed as mean \pm SEM. * $P < 0.05$, # $P < 0.01$.

Abbreviations: Emo, Emodin; LD-Emo, low-dose Emodin; HD-Emo, high-dose Emodin.

podocyte cytoskeletal protein, which is mainly expressed by the slit diaphragm of glomerular podocytes, and reduced expression of nephrin directly affects the morphology and function of podocytes. Previous studies have shown that the expression of nephrin was significantly decreased in rats with DN,^{27,28} contributing to the induction of proteinuria. In our study, the dramatically decreased nephrin expression in STZ-induced diabetic rats was significantly up-regulated by emodin. These results suggest that emodin could reduce proteinuria by up-regulating the expression of nephrin, thus protecting podocytes from damage induced by diabetes and delaying the progression of DN.

Autophagy is the process of removing the overall degradation of damaged proteins and organelles,⁴ which contributes to maintaining podocyte function. Under normal conditions, podocytes maintain a certain level of autophagy; in our experimental results, we observed a few autophagosomes in the Sham group. Previous research reports that insufficient autophagy in podocytes

was observed in DN rats, and massive proteinuria was accompanied by podocyte loss.²⁹ Consistently, our study shows that autophagosomes are absent in DN rats, and, after intervention by emodin, autophagosomes increased gradually, suggesting that autophagy has a self-stabilizing effect and plays a protective role in podocyte damage. To further confirm autophagy, we examined the expression of LC3-II as well as Beclin-1, which serve as valuable molecular biomarkers for the detection and assessment of autophagic activity, and the conversion of LC3-I to LC3-II is considered as a standard marker of autophagy.³⁰ Western blotting showed that, compared with the Sham group, the expression of LC3-II and Beclin-1 protein was significantly decreased in DN rats, and restored after emodin intervention. P62 protein (sequestosome 1, SQSTM1) is abbreviated as selective autophagy adaptor protein, which plays a variety of roles in the removal of cell selective autophagy and ubiquitinated protein. When autophagosomes combine with lysosomes to degrade content, p62 protein is largely consumed. Therefore, when

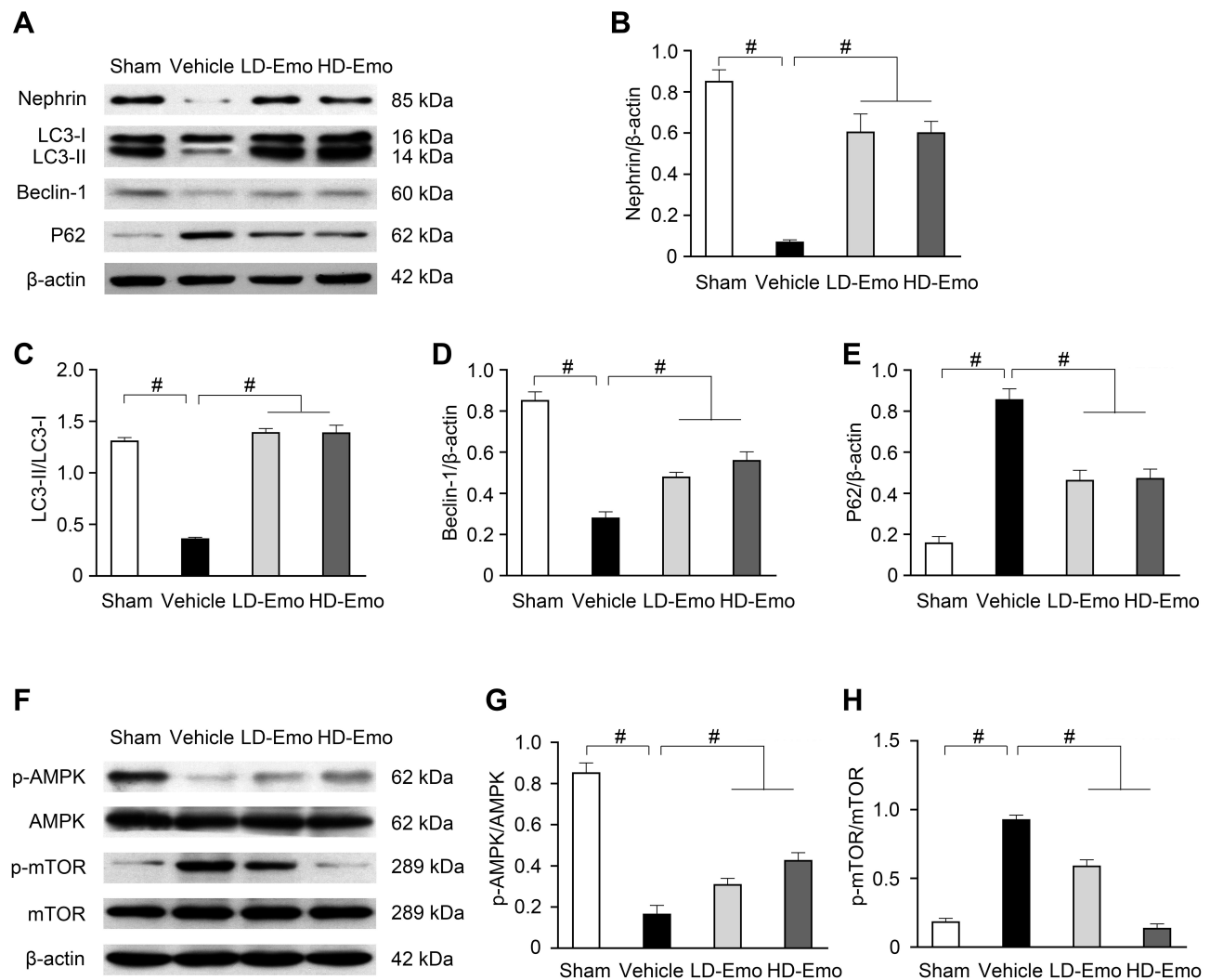


Figure 7 Effects of Emo on the protein expression of nephrin, LC3-II/I, Beclin-1, p62, p-AMPK, AMPK, p-mTOR and mTOR in the kidney.

Notes: (A) Western blot analysis of nephrin, LC3-II/I, Beclin-1 and p62 protein expression. (B–E) Quantitative analysis of nephrin, LC3-II/I, Beclin-1 and p62 protein expression. (F) Western blot analysis of p-AMPK, AMPK, p-mTOR and mTOR protein expression. (G and H) Quantitative analysis of p-AMPK and p-mTOR protein expression. Data are expressed as mean \pm SEM. # $P < 0.01$.

Abbreviations: Emo, Emodin; LD-Emo, low-dose Emodin; HD-Emo, high-dose Emodin; LC3, microtubule-associated protein 1 light-chain 3; P62 protein, p62/sequestosome-1 protein; AMPK, adenosine 5'-monophosphate (AMP)-activated protein kinase; p-AMPK, phospho-AMPK; mTOR, mammalian target of rapamycin; p-mTOR, phospho-mTOR.

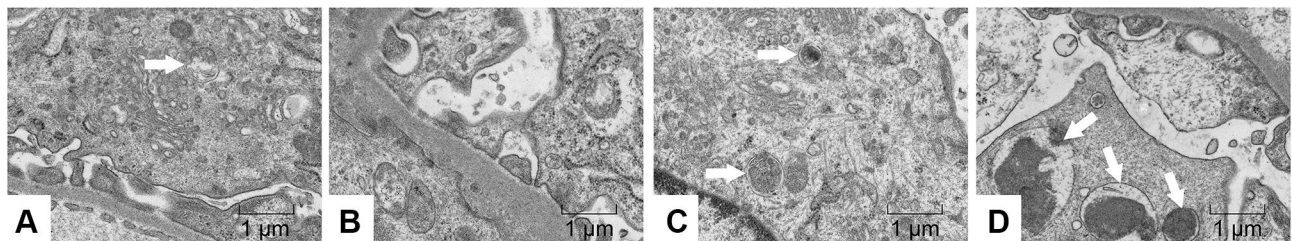


Figure 8 Effects of Emo on the autophagy of podocytes in rats with DN.

Notes: Electron microscopy (magnification, 15,000 \times). The white arrow indicates autophagosome. (A) Sham group, (B) Vehicle group, (C) LD-Emo group, (D) HD-Emo group.

Abbreviations: Emo, emodin; LD-Emo, low-dose emodin; HD-Emo, high-dose emodin.

a large amount of p62 protein is found to accumulate in the cell, it indicates that autophagy is in a suppressed state.³¹ In our study, Western blotting showed that p62 protein

expression is dramatically increased in DN rats, while obviously suppressed after emodin intervention. Collectively, these findings suggest that autophagy

activation is likely a kind of self-protection in dealing with diabetic stress in podocytes, and rescuing insufficient autophagy in podocytes under diabetic conditions plays an important role in the renoprotective effects of emodin.

The atypical serine/threonine protein kinase, mTOR, is a target protein of rapamycin, which can regulate cell growth and autophagy. In the state of adequate nutrition or without stress, mTOR is activated and autophagy is inhibited; however, when cells are in starvation or stress state under nutritional deficiency, mTOR activity is inhibited and autophagy is activated.³² Previous studies have shown that the pathogenesis of DN is related to autophagy inhibition induced by mTOR signaling pathway activation.³³ The mTOR signaling pathway is activated in the early stage of DN, and its over-activation can cause glomerular podocyte damage. Strict control of mTOR activity is the key to maintaining glomerular podocyte function. AMPK is an important serine/threonine protein kinase, which is one of the upstream pathways of mTOR. Under the condition of ischemia and hypoxia, the nutrient deficiency and ATP level decreased, activation of AMPK leads to the phosphorylation and activation of TSC1/2 complex, which can indirectly inhibit mTOR activity by inhibiting rheb enzyme activity, or directly phosphorylate Raptor, a subunit of mTORC1, to inhibit mTOR, thus enhancing autophagy.¹⁸ Studies have shown that the phosphorylation of AMPK was inhibited in the kidney tissue of DN; in STZ-induced diabetic rats, the addition of AMPK agonists can significantly increase the phosphorylation of AMPK, thus reducing kidney damage and proteinuria.^{34,35} In STZ-induced diabetic mice, the activation of AMPK can reduce podocyte apoptosis and proteinuria, suggesting that the activation of AMPK may be involved in the protection of podocytes.³⁶ In our study, we found that emodin significantly increased p-AMPK protein levels and inhibited p-mTOR protein levels in the kidneys of STZ-induced diabetic rats, indicating that emodin enhanced autophagy by increasing AMPK protein levels. In addition, a previous study has shown that emodin can improve dyslipidemia in rats fed with high-fat diet by activating AMPK.²¹ Currently, our data show that emodin up-regulated AMPK phosphorylation and down-regulated mTOR phosphorylation, suggesting that emodin might positively regulate the autophagic process.

Cellular apoptosis, especially podocyte apoptosis, plays an important role in renal diseases. As terminally differentiated cells, podocytes lack repair capacity and regeneration potency after damage. Under the stimulation

of various stress factors in the process of DN, a large number of damaged proteins and organelles accumulate in podocytes, which will lead to podocyte loss and podocyte apoptosis. Decrease in the number of podocytes causes proteinuria, and finally results in glomerular sclerosis.^{37,38} It has been shown that the expression of pro-apoptotic proteins (Bax and Cleaved caspase-3) was increased in DN rats. In the current study, DN rats exhibited increased expression of Bax and Cleaved caspase-3, which were significantly reduced by emodin intervention. The effect of emodin on cellular apoptosis was also confirmed by TUNEL staining. The number of apoptotic glomerular and tubular epithelial cells was significantly increased in the Vehicle group, which was significantly improved after the intervention with emodin. These results indicate that emodin can reduce the STZ-induced glomerular and tubular epithelial cell apoptosis.

Conclusion

Our results demonstrated that emodin, as a natural regulator in vivo, reduced proteinuria and alleviated renal fibrosis without affecting hyperglycemia in DN rats. The potential mechanisms by which emodin exerts its renoprotective effects in vivo are through suppressing cell apoptosis and enhancing autophagy of podocytes via the AMPK/mTOR signaling pathway in the kidney. These findings provide new insights into the molecular mechanisms underlying the renoprotective effects of emodin in DN.

Acknowledgments

This study was supported by the Chinese Medicine Research Project of Hubei Provincial Health Commission (grant number: ZY2019Q024), National Natural Science Foundation of China (grant number: 81503432) and Natural Science Foundation of Hubei Province (grant number: 2015CFB395).

Disclosure

The authors report no conflicts of interest in this work.

References

1. Van Buren PN, Toto R. Current update in the management of diabetic nephropathy. *Curr Diabetes Rev*. 2013;9(1):62–77. doi:10.2174/157339913804143207
2. Li JJ, Kwak SJ, Jung DS, et al. Podocyte biology in diabetic nephropathy. *Kidney Int Suppl*. 2007;72(106):S36–42. doi:10.1038/sj.ki.5002384

3. Ristola M, Lehtonen S. Functions of the podocyte proteins nephrin and Neph3 and the transcriptional regulation of their genes. *Clin Sci*. 2013;126(5):315–328. doi:10.1042/CS20130258
4. Mizushima N, Komatsu M. Autophagy: renovation of cells and tissues. *Cell*. 2011;147(4):728–741. doi:10.1016/j.cell.2011.10.026
5. Kim WY, Nam SA, Song HC, et al. The role of autophagy in unilateral ureteral obstruction rat model. *Nephrology (Carlton)*. 2012;17(2):148–159. doi:10.1111/j.1440-1797.2011.01541.x
6. Yadav A, Vallabu S, Arora S, et al. ANG II promotes autophagy in podocytes. *Am J Physiol Cell Physiol*. 2010;299(2):C488–496. doi:10.1152/ajpcell.00424.2009
7. Liu H, Gu LB, Tu Y, Hu H, Huang YR, Sun W. Emodin ameliorates cisplatin-induced apoptosis of rat renal tubular cells in vitro by activating autophagy. *Acta Pharmacol Sin*. 2016;37(2):235–245. doi:10.1038/aps.2015.114
8. Wang HH, Chung JG. Emodin-induced inhibition of growth and DNA damage in the *Helicobacter pylori*. *Curr Microbiol*. 1997;35(5):262–266. doi:10.1007/s002849900250
9. Chang CH, Lin CC, Yang JJ, Namba T, Hattori M. Anti-inflammatory effects of emodin from ventral leiocarpa. *Am J Chin Med*. 1996;24(2):139–142. doi:10.1142/S0192415X96000189
10. Yon JM, Baek IJ, Lee BJ, Yun YW, Nam SY. Emodin and [6]-gingerol lessen hypoxia-induced embryotoxicities in cultured mouse whole embryos via upregulation of hypoxia-inducible factor 1 α and intracellular superoxide dismutases. *Reprod Toxicol*. 2011;31(4):513–518. doi:10.1016/j.reprotox.2011.02.011
11. Huang HC, Chang JH, Tung SF, Wu RT, Foegh ML, Chu SH. Immunosuppressive effect of emodin, a free radical generator. *Eur J Pharmacol*. 1992;211(3):359–364. doi:10.1016/0014-2999(92)90393-1
12. Zhang CC, Meng FX, He Y, Wang DL, Wang J. Effect of the Emodin on TGF- β 1/CTGF signaling pathway in kidney of diabetic nephropathy model rats. *Adv Integr Med*. 2019;6(1):S149–151.
13. Chang YC, Lai TY, Yu CS, et al. Emodin induces apoptotic death in murine myelomonocytic leukemia WEHI-3 cells in vitro and enhances phagocytosis in leukemia mice in vivo. *Evid Based Complement Alternat Med*. 2011;2011(3):523–596. doi:10.1155/2011/523596
14. Wang J, Huang H, Liu P, et al. Inhibition of phosphorylation of p38 MAPK involved in the protection of nephropathy by emodin in diabetic rats. *Eur J Pharmacol*. 2006;553(1–3):297–303. doi:10.1016/j.ejphar.2006.08.087
15. Li X, Liu W, Wang Q, et al. Emodin suppresses cell proliferation and fibronectin expression via p38MAPK pathway in rat mesangial cells cultured under high glucose. *Mol Cell Endocrinol*. 2009;307(1–2):157–162. doi:10.1016/j.mce.2009.03.006
16. Chen T, Zheng LY, Xiao W, Gui D, Wang X, Wang N. Emodin ameliorates high glucose induced-podocyte epithelial-mesenchymal transition in-vitro and in-vivo. *Cell Physiol Biochem*. 2015;35(4):1425–1436. doi:10.1159/000373963
17. Kitada M, Takeda A, Nagai T, Ito H, Kanasaki K, Koya D. Dietary restriction ameliorates diabetic nephropathy through anti-inflammatory effects and regulation of the autophagy via restoration of Sirt1 in diabetic Wistar fatty (fa/fa) rats: a model of type 2 diabetes. *Exp Diabetes Res*. 2011;2011:908185. doi:10.1155/2011/908185
18. Kim J, Kundu M, Viollet B, Guan K-L. AMPK and mTOR regulate autophagy through direct phosphorylation of Ulk1. *Nat Cell Biol*. 2011;13(2):132–141. doi:10.1038/ncb2152
19. Song P, Kim JH, Ghim J, et al. Emodin regulates glucose utilization by activating AMP-activated protein kinase. *J Biol Chem*. 2013;288(8):5732–5742. doi:10.1074/jbc.M112.441477
20. Mao ZM, Shen SM, Wan YG, et al. Huangkuai capsule attenuates renal fibrosis in diabetic nephropathy rats through regulating oxidative stress and p38MAPK/Akt pathways, compared to α -lipoic acid. *J Ethnopharmacol*. 2015;173:256–265. doi:10.1016/j.jep.2015.07.036
21. Tzeng TF, Lu HJ, Liou SS, Chang CJ, Liu IM. Emodin, a naturally occurring anthraquinone derivative, ameliorates dyslipidemia by activating AMP-activated protein kinase in high-fat-diet-fed rats. *Evid Based Complement Alternat Med*. 2012;2012:781812. doi:10.1155/2012/781812
22. Yang X, Ma LB, Xie XC, et al. Effect of Emodin on the expressions of MMP-2/TIMP-2 in the renal tissue of rats with diabetes. *Chin J Diabetes*. 2016;24(2):159–162.
23. Zandi-Nejad K, Eddy AA, Glasscock RJ, Brenner BM. Why is proteinuria an ominous biomarker of progressive kidney disease? *Kidney Int Suppl*. 2004;66(92):S76–89. doi:10.1111/j.1523-1755.2004.09220.x
24. Kerjaschki D. Caught flat-footed: podocyte damage and the molecular bases of focal glomerulosclerosis. *J Clin Invest*. 2001;108(11):1583–1587. doi:10.1172/JCI200114629
25. Pagtalunan ME, Miller PL, Jumping-Eagle S, et al. Podocyte loss and progressive glomerular injury in type II diabetes. *J Clin Invest*. 1997;99(2):342–348. doi:10.1172/JCI119163
26. Weil EJ, Lemley KV, Mason CC, et al. Podocyte detachment and reduced glomerular capillary endothelial fenestration promote kidney disease in type 2 diabetic nephropathy. *Kidney Int*. 2012;82(9):1010–1017. doi:10.1038/ki.2012.234
27. Hu Y, Ye S, Xing Y, Lv L, Hu W, Zhou W. Saxagliptin attenuates glomerular podocyte injury by increasing the expression of renal nephrin and podocin in type 2 diabetic rats. *Acta Diabetol*. 2020;57(3):279–286. doi:10.1007/s00592-019-01421-7
28. Aaltonen P, Luimula P, Astrom E, et al. Changes in the expression of nephrin gene and protein in experimental diabetic nephropathy. *Lab Invest*. 2001;81(9):1185–1190. doi:10.1038/labinvest.3780332
29. Liu S, Hartleben B, Kretz O, et al. Autophagy plays a critical role in kidney tubule maintenance, aging and ischemia-reperfusion injury. *Autophagy*. 2012;8(5):826–837. doi:10.4161/auto.19419
30. Tanida I, Ueno T, Kominami E. LC3 conjugation system in mammalian autophagy. *Int J Biochem Cell Biol*. 2004;36(12):2503–2518. doi:10.1016/j.biocel.2004.05.009
31. Dall'Armi C, Devereaux KA, Di Paolo G. The role of lipids in the control of autophagy. *Curr Biol*. 2013;23(1):R33–45. doi:10.1016/j.cub.2012.10.041
32. Hosokawa N, Hara T, Kaizuka T, et al. Nutrient-dependent mTORC1 association with the ULK1-Atg13-FIP200 complex required for autophagy. *Mol Biol Cell*. 2009;20(7):1981–1991. doi:10.1091/mbc.e08-12-1248
33. Dunlop EA, Hunt DK, Acosta-Jaquez HA, Fingar DC, Tee AR. ULK1 inhibits mTORC1 signaling, promotes multisite Raptor phosphorylation and hinders substrate binding. *Autophagy*. 2011;7(7):737–747. doi:10.4161/auto.7.7.15491
34. Lee JW, Park S, Takahashi Y, Wang HG. The association of AMPK with ULK1 regulates autophagy. *PLoS One*. 2010;5(11):e15394. doi:10.1371/journal.pone.0015394
35. Mihaylova MM, Shaw RJ. The AMPK signalling pathway coordinates cell growth, autophagy and metabolism. *Nat Cell Biol*. 2011;13(9):1016–1023. doi:10.1038/ncb2329
36. Zhou D, Zhou M, Wang Z, et al. Progranulin alleviates podocyte injury via regulating CAMKK/AMPK-mediated autophagy under diabetic conditions. *J Mol Med (Berl)*. 2019;97(11):1507–1520. doi:10.1007/s00109-019-01828-3
37. Kriz W. Podocyte is the major culprit accounting for the progression of chronic renal disease. *Microsc Res Tech*. 2002;57(4):189–195. doi:10.1002/jemt.10072
38. Mundel P, Shankland SJ. Podocyte biology and response to injury. *J Am Soc Nephrol*. 2002;13(12):3005–3015. doi:10.1097/OI.ASN.0000039661.06947.FD

Diabetes, Metabolic Syndrome and Obesity: Targets and Therapy

Dovepress

Publish your work in this journal

Diabetes, Metabolic Syndrome and Obesity: Targets and Therapy is an international, peer-reviewed open-access journal committed to the rapid publication of the latest laboratory and clinical findings in the fields of diabetes, metabolic syndrome and obesity research. Original research, review, case reports, hypothesis formation, expert opinion

and commentaries are all considered for publication. The manuscript management system is completely online and includes a very quick and fair peer-review system, which is all easy to use. Visit <http://www.dovepress.com/testimonials.php> to read real quotes from published authors.

Submit your manuscript here: <https://www.dovepress.com/diabetes-metabolic-syndrome-and-obesity-targets-and-therapy-journal>